

Immunoglobulins on the surface of differently charged polymer nanoparticles F

Cite as: Biointerphases **15**, 031009 (2020); <https://doi.org/10.1116/6.0000139>

Submitted: 20 February 2020 . Accepted: 26 April 2020 . Published Online: 01 June 2020

Domenik Prozeller , Christine Rosenauer, Svenja Morsbach , and Katharina Landfester 

COLLECTIONS

Paper published as part of the special topic on [Special Topic Collection: Protein Corona at Nanointerfaces](#)

Note: This paper is part of the Biointerphases Special Topic Collection on Protein Corona at Nanointerfaces.

F This paper was selected as Featured



View Online



Export Citation



CrossMark

ARTICLES YOU MAY BE INTERESTED IN

[Interactions with charged surfaces affect antibody behavior](#)

Scilight **2020**, 231102 (2020); <https://doi.org/10.1063/10.0001373>

[Linear wormlike micelles exhibit behaviors similar to ordinary polymers in strong saline flows](#)

Scilight **2020**, 231103 (2020); <https://doi.org/10.1063/10.0001407>

[Additive manufacture of photonic components for the terahertz band](#)

Journal of Applied Physics **127**, 210901 (2020); <https://doi.org/10.1063/1.5140270>



NEW

AVS Quantum Science

A new interdisciplinary home for impactful quantum science research and reviews

Co-Published by



NOW ONLINE

Immunoglobulins on the surface of differently charged polymer nanoparticles



Cite as: *Biointerphases* 15, 031009 (2020); doi: 10.1116/6.0000139

Submitted: 20 February 2020 · Accepted: 26 April 2020 ·

Published Online: 1 June 2020



View Online



Export Citation



CrossMark

Domenik Prozeller, Christine Rosenauer, Svenja Morsbach,^{a)} and Katharina Landfester

AFFILIATIONS

Max Planck Institute for Polymer Research, Ackermannweg 10, 55128 Mainz, Germany

Note: This paper is part of the *Biointerphases* Special Topic Collection on Protein Corona at Nanointerfaces.

^{a)}Electronic mail: morsbachs@mpip-mainz.mpg.de

ABSTRACT

The overall success of nanocarriers in biomedical applications depends on their interaction with different proteins in blood. Immunoglobulins as a major protein class of the blood proteome may considerably influence the identity of the nanocarriers in blood. However, there is a lack of knowledge about the specific details of the interaction mechanism between different immunoglobulins and nanocarriers. Therefore, the authors have investigated the interaction of different immunoglobulin classes—namely, immunoglobulin G, A, and M—with different polystyrene model nanoparticles. The authors report that immunoglobulin interaction with nanoparticles strongly depends on the immunoglobulin class and surface charge of the nanoparticles. Furthermore, upon adsorption on the nanoparticles' surfaces, aggregation processes and denaturation of immunoglobulins were observed. This highlights the importance of nanocarriers' design in order to prevent unfavorable denaturation and adsorption processes of immunoglobulins on nanoparticle surfaces.

© 2020 Author(s). All article content, except where otherwise noted, is licensed under a Creative Commons Attribution (CC BY) license (<http://creativecommons.org/licenses/by/4.0/>). <https://doi.org/10.1116/6.0000139>

I. INTRODUCTION

The desired overall success of nanocarriers (NCs) in medicine strongly depends on the interactions that NCs undergo in the organism. If NCs are introduced into the blood circulation by intravenous injections, proteins will adsorb on the NCs' surface resulting in the formation of the so-called protein corona.^{1–4} This protein corona can be more or less pronounced, consists of different protein fractions depending on favored interactions, and results in pronounced differences of cellular uptake of nanocarriers.^{5–8}

One major protein class and significant part of blood proteome are immunoglobulins (Igs). The Ig concentration averages around 16 g l^{-1} with a total protein concentration in human blood of around $60\text{--}70 \text{ g l}^{-1}$ for adults.⁹ The major Ig classes of the proteome consist of IgG at a concentration of approximately $11\text{--}12 \text{ g l}^{-1}$, IgA at a concentration of 2.6 g l^{-1} , and IgM at a concentration of 1.5 g l^{-1} on average.¹⁰

As the name already implies, immunoglobulins generally play an important role in the immune system. Interactions of Igs with any compound foreign to the organism, including biomedical NCs, trigger the recognition of Igs by cells of the immune system (e.g., macrophages) resulting in immune cascades ultimately leading to

the clearance of these foreign compounds from the organism.¹¹ Therefore, interactions between NCs and immunoglobulins could potentially result in unwanted behavior of the NCs inside the body, such as (auto)immune reactions, inflammation, and allergic reactions, mainly by inducing complement activation.^{12–14} Furthermore, Igs behave as opsonins in the protein corona of NCs, which means they lead to unspecific cell uptake resulting in a significantly decreased circulation time *in vivo*.^{15,16} Recently, we found that nanocarriers even significantly adsorb more immunoglobulins in Ig-enriched plasma (as found in diseased patients) leading to enhanced unspecific cell uptake.¹⁷ Following this, the role of the different Igs in the protein corona of nanocarriers is of importance. Their interaction mechanism has to be fully understood in order to minimize NC-Ig interactions as much as possible, resulting in a better chance that NCs will not be cleared by the immune system or even induce adverse effects.

While some studies about immunoglobulin adsorption were also conducted on flat surfaces with regard to charge effects, ion concentrations and *pH* (Ref. 18), as well as surface hydrophobicity,¹⁹ still more investigations are needed concerning the prediction of interaction with nanomaterials.

For example, the adsorption behavior of individual Ig classes, such as IgG, on different NCs was found to be independent of the NC size or surface curvature in general,^{20,21} but the influence of NCs' surface charge on the adsorption mechanism of the different Ig classes is still under investigation. In order to draw general conclusions for interaction trends between Igs and differently charged NCs, model NCs with different physicochemical properties are needed. For this we used polystyrene nanoparticles (PS-NPs) with different functional groups (unfunctionalized, carboxy-functionalized, and amino-functionalized) as model systems for the investigation of interactions with IgG, IgA, and IgM from human plasma. The adsorption of different immunoglobulin classes on the surface of NCs was confirmed via sodium dodecyl sulfate polyacrylamide gel electrophoresis (SDS-PAGE). By investigating the respective zeta potential (ζ), the influence of Igs on the apparent charge of differently charged nanoparticles was analyzed. Furthermore, the thermodynamic adsorption parameters of the respective interactions were analyzed via isothermal titration calorimetry (ITC). Analysis of the Ig's influence on the stability and aggregation tendency of NCs was performed via dynamic light scattering (DLS). Additionally, the structural stability of immunoglobulins after adsorption was analyzed via nanodifferential scanning fluorimetry (nanoDSF).

II. EXPERIMENT

A. Materials

IgG (product no. I4506), IgA (product no. I4036), and IgM (product no. I8260) from human serum were purchased from Sigma Aldrich (St. Louis, USA) and used without further purification. All three of the herein used NCs were synthesized using the miniemulsion (co)polymerization method with styrene and comonomers [acrylic acid in the case of carboxylic nanoparticles or 2-aminoethyl methacrylate hydrochloride (AEMH) in the case of amino-functionalized nanoparticles] and Lutensol AT50 [a poly(ethylene oxide)-hexadecyl ether with an ethyleneoxide length of about 50 units] as surfactant as previously published.²² In brief, a mixture of styrene, the respective comonomer, initiator 2,20-azobis(2-methylbutyronitrile) (V59, Wako Chemicals), hydrophobe (hexadecane), and N-(2,6-diisopropylphenyl)-perylene-3,4-dicarboximide (PMI, BASF) was added to the aqueous phase containing Lutensol AT50. After 1 h of pre-emulsification, the mixture was sonicated [Branson Sonifier (1/2 in. tip, 6.5 mm diameter) for 2 min at 450 W and 90% amplitude] in an ice-cold bath. The copolymerization was carried out at 72 °C at 1000 rpm. The resulting NPs were washed five times via centrifugation and resuspension in Milli-Q water. Minimal amounts of surfactant remained in the nanoparticle dispersion for preventing agglomeration of the nanomaterials. The used nanoparticles were filtered through Millex-SV 5 μ m filters (Merck Millipore, Billerica, USA) before use in order to remove aggregates or potential impurities like dust.

B. Protein corona preparation

For each sample, an aqueous nanoparticle suspension (0.05 m² of surface area in a total volume of 300 μ L) was mixed in an Eppendorf-tube with 1 ml solution (1 g l⁻¹) of the respective immunoglobulin in phosphate-buffered saline (PBS). After 1 h of mild

shaking at 37 °C, the sample was centrifuged for 1 h at 20 000 g and 4 °C. The supernatant was discarded and the pellet resuspended in 1 ml of PBS. The suspension was again centrifuged for 1 h at 20 000 g and 4 °C. These washing steps were repeated for a total of three times. Before the last washing step, the suspension was transferred into a new Eppendorf-tube. After the last washing step, the pellet was resuspended in 1 ml of Milli-Q water.

C. SDS-PAGE

After the last washing step of the corona preparation (see above), the pellet was suspended in 100 μ l of a 62.5 mM Tris*HCl solution containing 2% SDS. The suspension was incubated at 95 °C for 5 min and was centrifuged for 1 h at 20 000 g and 4 °C. The protein concentration of each sample was determined using a Pierce 660 nm Assay Kit by ThermoFisher (Waltham, USA) with bovine serum albumin as standard reagent as described by the manufacturer. 26 μ l of the supernatant containing 6 μ g of the desorbed proteins according to the previously performed Pierce assay were mixed with 4 μ l of reducing agent and 10 μ l of sample buffer. Fresh immunoglobulin solutions were used as reference samples. After 1 h at 100 V, the electrophoresis was stopped. Staining was performed using a ready-to-use Coomassie Brilliant Blue (SimplyBlue SafeStain) staining solution for 2 h and destained in Milli-Q water over night. In the case of nonreducing SDS-PAGE [see supplementary material (Ref. 34)], 4 μ l of the reducing agent in the procedure described above is replaced by Milli-Q water.

D. Zeta potential

Zeta potential measurements were performed using a Nano Z Zetasizer (Malvern Instruments GmbH, Herrenberg, Germany). 20 μ l of the samples (pure nanoparticle suspensions, pure protein solutions, and NP-protein complexes after centrifugation and resuspension, respectively) were diluted with 1 ml of a 1 mM KCl solution and measured instantly at 25 °C after 2 min of equilibration. Each measurement was repeated in triplicate and mean values as well as standard deviations were calculated.

E. ITC

ITC measurements were performed using a NanoITC Low Volume (TA Instruments, Eschborn, Germany) with an effective cell volume of 170 μ l. During each experiment, 50 μ l of the respective immunoglobulin [$c(\text{IgG}) = 10 \text{ g l}^{-1}$ ($6.7 \cdot 10^{-2} \text{ mM}$), $c(\text{IgA}) = 1.1 \text{ g l}^{-1}$ ($6.9 \cdot 10^{-3} \text{ mM}$), and $c(\text{IgM}) = 0.1 \text{ g l}^{-1}$ ($1.0 \cdot 10^{-4} \text{ mM}$) in PBS] were titrated into 300 μ l of an aqueous suspension of the respective NCs; for titrations with IgG: $c(\text{NCs}) = 19 \text{ g l}^{-1}$; for titrations with IgA: $c(\text{NCs}) = 1.9 \text{ g l}^{-1}$; for titrations with IgM: $c(\text{NCs}) = 6.0 \text{ g l}^{-1}$. Additionally, the same amount of immunoglobulin solution was titrated into 300 μ l of ultrapure water for determining the dilution heat for reference. The number of injections was set to 25 for each measurement (25 \times 2 μ l) with a spacing of 250 s between every injection. Each measurement was carried out at 15 °C. The integrated heats of dilution were subtracted from the integrated heats of every adsorption measurement. The normalized heats were fitted according to an independent binding model [see eq. (S1)]³⁴ to obtain the association constant (K_a), the reaction enthalpy (ΔH), the entropy

TABLE I. Characterization of NC systems regarding physicochemical properties.

	PS-NPs	PS-NPs-COOH	PS-NPs-NH ₂
Material	Polystyrene (PS)	Polystyrene (PS)	Polystyrene (PS)
Surfactant	Lutensol AT50	Lutensol AT50	Lutensol AT50
Functional group	None	carboxy (–COOH)	amino (–NH ₂)
R _h /nm	52 ± 5	57 ± 6	51 ± 5
Zeta potential ζ/mV	–10 ± 1	–29 ± 2	2 ± 1

(ΔS), the Gibbs free energy (ΔG), and the reaction stoichiometry (*n*). Each measurement was carried out in triplicate and the mean value as well as standard deviation for each parameter were calculated. Data evaluation of the ITC measurements was performed using the NANO ANALYZE Data Analysis Software (Software version 3.6.0) from TA Instruments.

F. Surface charge mapping of immunoglobulins

Crystal structures of IgG and IgA-F_c were downloaded from www.rcsb.org [PDB ID (IgG): 1IGT; PDB ID (IgA-F_c): 1OW0]. The crystal structure of the IgM-F_c domain [PDB ID (IgM-F_c): 1O0V] was generated via homology modeling with the SWISS-MODEL server (<http://swissmodel.expasy.org/>) using the template with the highest quality (1o0v.1.B). The IgM-F_c model was calculated based on the target-template alignment via energy minimization using the fully integrated protein structure prediction program PRIME (Schrödinger LLC, New York, NY) in a similar fashion to the recent publication by Hiramoto *et al.*²³ Images of the crystal structures depicting surface charge mapping were created utilizing the software “MOLECULAR OPERATING ENVIRONMENT” (MOE 2019.01). The energy of the 3D structures was minimized applying the MMFF94x force field before plotting the surface map. Red areas in the graphics represent negatively charged patches, while blue areas represent positively charged patches and white areas are of neutral charge.

G. DLS

DLS measurements were performed using an instrument from ALV (Langen, Germany) consisting of an electronically controlled goniometer and an ALV-5000 multiple τ full-digital correlator with 320 channels with a measurement range between 10^{–7} and 10³ s. A helium-neon laser (Type 1145 P) from JDS Uniphase (Milpitas, USA) of 632.8 nm wavelength and 25 mV output power was used as a source of light. Before measurements, Milli-Q water was filtered into quartz cuvettes for light scattering from Hellma (Müllheim, Germany), applying Millex-GS filters (Merck Millipore, Billerica, USA) with 220 nm pore size. Afterward, 2 μl of NPs and/or 10 μl of Ig were added into the cuvette and incubated for 10 min at room temperature before measurement. Prior to use, the quartz cuvettes were cleaned with acetone using a Thurmond apparatus.²⁴ The method by Rausch *et al.*²⁵ has been applied for analysis of DLS experiments. Further details on the data analysis can be found in the supplementary material.³⁴

H. NanoDSF

NanoDSF measurements of immunoglobulin solutions with or without the presence of NCs were performed using a NanoDSF Prometheus NT.48 device with standard capillaries (NanoTemper Technologies, München, Germany). The immunoglobulin concentration in each sample containing immunoglobulins was 1.0 g l^{–1} in PBS. Analysis and online monitoring of the DSF measurement was performed using the PR.CONTROLL Data Analysis Software (v1.12.3) from NanoTemper Technologies. Fluorescence of each sample was analyzed at wavelengths of 350 and 330 nm. The temperature was increased from 20.0 to 95.0 °C at a rate of 0.5 °C min^{–1}.

III. RESULTS AND DISCUSSION

In this study, the interactions between Igs and different NCs were investigated. For this, dispersions of the respective NC were incubated with solutions of the respective Ig in PBS. In order to be able to draw conclusions between the resulting Ig-NC interaction and the surface charge of NCs, different model NCs were used in this study (see Table I). All NCs used are polystyrene nanoparticles stabilized by minimal amounts of a poly(ethylene glycol) based surfactant (Lutensol AT50) and share similar hydrodynamic radii between 50 and 60 nm in order to exclude influences of these parameters. However, different surface functionalities were created by using different comonomers throughout the miniemulsion polymerization in order to achieve differently charged NCs. The resulting polystyrene nanoparticles used were unfunctionalized (PS-NPs), carboxy-functionalized (PS-NPs-COOH) by using acrylic acid as a comonomer, or amino-functionalized (PS-NPs-NH₂) by using AEMH as a comonomer.

First, the presence of Ig chains on the surface of the different PS-NPs was investigated via a reducing SDS-PAGE. For that purpose, different NPs were incubated with each individual Ig type and subsequently separated from free proteins by repeated washing steps. The remaining proteins were detached from the NPs by incubation with SDS and were analyzed afterward. The identified protein patterns are shown in Fig. 1. The different light and heavy chains of immunoglobulins can be found on the surface of the different PS-NPs and show distinct bands because the connecting disulfide bridges were cleaved during the reducing conditions. Visible differentiation between the different Igs is possible by analyzing the molar weight corresponding to the bands of the heavy chains (between 50 and 70 kDa), while light chains share the same molecular weight around 25 kDa.

Additionally, analyzing the antibodies without reduction step prior to electrophoresis is depicted in the supplementary material

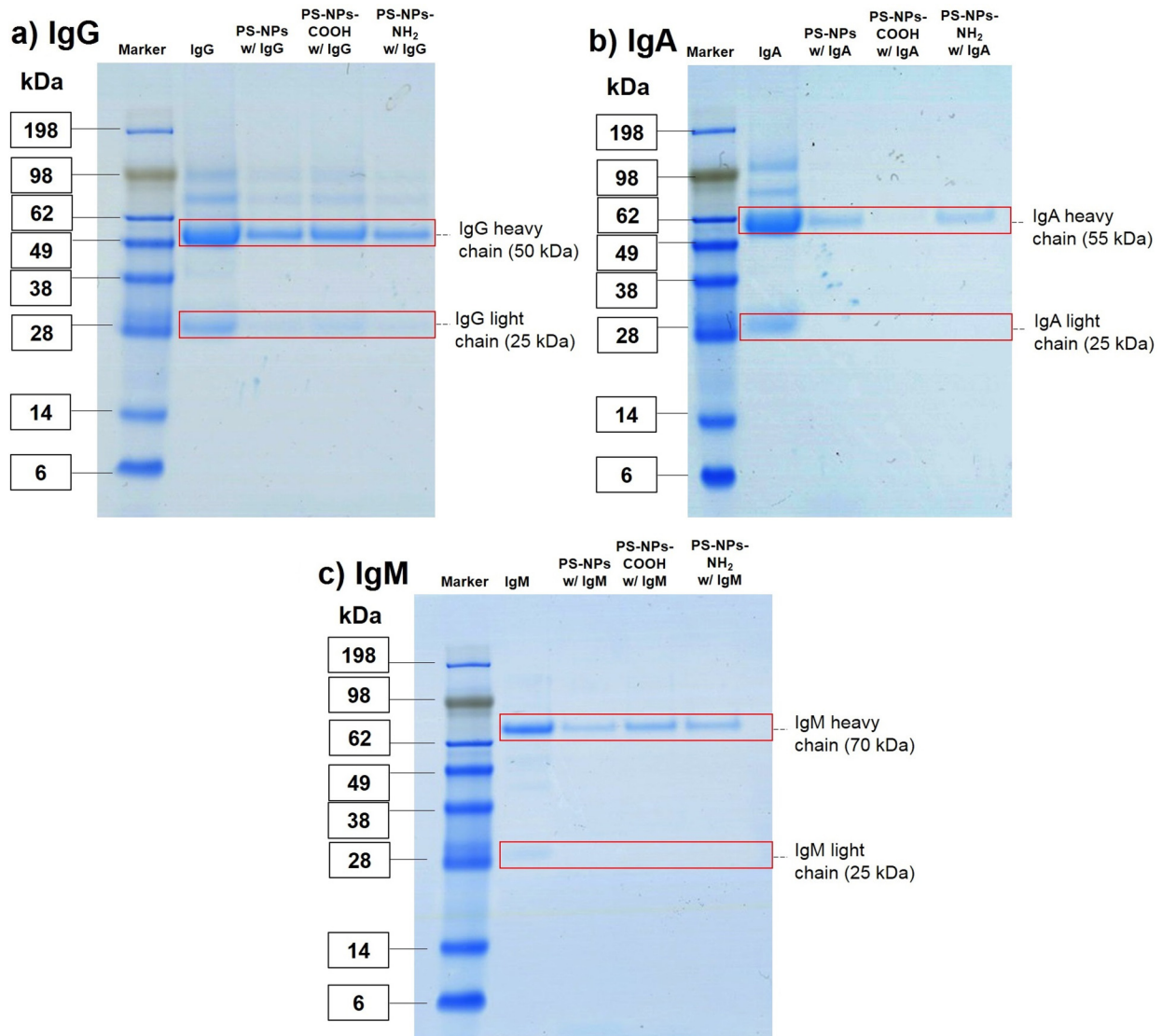


FIG. 1. Reducing SDS-PAGE gel of the protein corona of PS-NPs incubated with (a) IgG, (b) IgA, and (c) IgM. Pure Igs are shown as a reference. For staining, a ready to use Coomassie staining solution was used according to the manufacturer's instruction.

(see Fig. S1).³⁴ Comparing reduced and nonreduced bands gives further information on the original structure of the respective immunoglobulin. IgG and IgA have similar molar weights of around 150 kDa in the nonreduced SDS-PAGE implying monomeric immunoglobulins. However, they can be distinguished by the difference in the molar weight of the heavy chains (50 kDa for IgG and 55 kDa for IgA). IgM appears with a significantly higher molar weight (≈ 1000 kDa) in the nonreduced SDS-PAGE, which is explained by the pentameric nature of IgM. In summary, all Igs can be found on the surface of each NP sample, while the interaction between IgA and the three different NPs appears to be rather

weak, especially in the case of PS-NPs-COOH. However, a determination of the interaction mechanism cannot be achieved from these results obtained via SDS-PAGE. In order to achieve more information on the interaction mechanism, the influence of the NP surface charge was investigated concerning the net charge of the Igs and the subsequent interaction of both using zeta potential measurements (see Fig. 2).

According to Fig. 2, Igs themselves exhibit different zeta potentials in accordance with their isoelectric points reported in literature [$pI(\text{IgG}) = \text{pH } 7-9.95$; $pI(\text{IgA}) = \text{pH } 4.7-5.9$; $pI(\text{IgM}) = \text{pH } 5.5-6.7$].²⁶ While the overall surface charge for IgG is almost

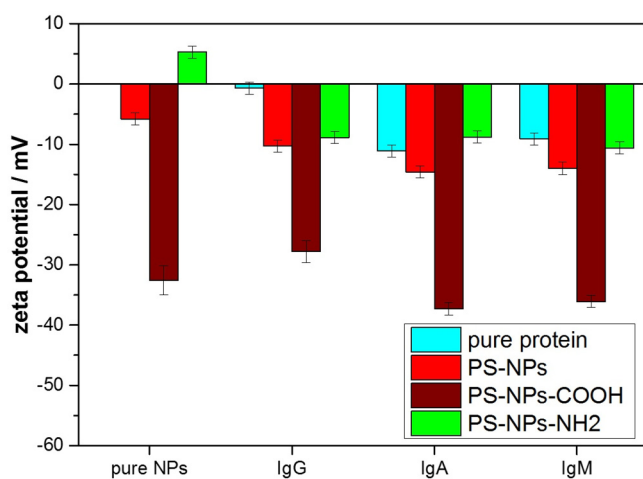


FIG. 2. Bar diagrams for the zeta potentials of the different pure PS-NPs and Igs as well as zeta potentials of the different PS-NPs after incubation with the different Igs and washing at pH = 7 in 1mM KCl.

neutral at pH 7, IgA and IgM overall are slightly negatively charged. The pure PS-NPs themselves (left columns) differ in zeta potential in accordance with their surface charge as well, with PS-NPs-COOH exhibiting a much more negative zeta potential than unfunctionalized PS-NPs and PS-NPs-NH₂ with a positive zeta potential. Adsorbed IgG leads to a more negative zeta potential of PS-NPs-NH₂. While IgA and IgM show a negative zeta potential in their native state, all NPs (especially amino-functionalized ones) exhibit a more negative zeta potential after incubation with IgA and IgM. Carboxy-functionalized NPs, which are already highly negatively charged, interestingly keep their surface charge. Because the net charge of the immunoglobulins is less negative than the one of the nanoparticles, one could expect that upon formation of a dense thick protein layer, the zeta potential of the complex approaches one of the native proteins, if the charged carboxyl groups are not exposed to the outside anymore. However, this was not the case, which indicates that the initial charges were still accessible to a certain extent and could mean that the protein layer was not particularly dense and/or uniform. These measurements already indicate that the different Ig types interact differently with certain charged or non-charged surfaces.

Upon further investigation of the adsorption process of Igs onto NCs, the thermodynamic parameters of the respective interaction were investigated via ITC. For that, all NP types were titrated with solutions of the different Igs and the corresponding heat of interaction was analyzed. The obtained heat rates are shown in Figs. S2–S10 (Ref. 34), and their corresponding adsorption isotherms are displayed in Fig. 3. All adsorption isotherms were fitted according to an independent binding model where possible. The obtained adsorption parameters are summarized in Table II. It has to be noted that all titrations were performed at 15 °C. At higher temperatures, no changes in heat

were visible, although interaction was already confirmed by SDS-PAGE. This means that interactions were heat-neutral at higher temperature.

The adsorption behavior of the different Igs on the different NCs is very different (see Fig. 3 and Table II). While the adsorption processes of IgG produces enough heat for obtaining thermodynamic data by independent binding fits, for IgA and IgM, almost no heat change is observed during titration. This could be due to relatively weak interactions between the NPs and IgA or IgM, respectively (as discussed above via SDS-PAGE) or it could be due to the limitation of the protein concentration in the protein source. Only in the case of interaction between PS-NPs-COOH and IgM, a large amount of heat was registered. In the case of IgG, the interaction with all PS-NPs is differently enthalpy driven. PS-NPs without functional groups on the surface exhibit the highest affinity toward IgG and in relation with the smallest enthalpy gain as well as entropy loss. PS-NPs-COOH, on the other hand, shows the least affinity toward IgG and the most enthalpy-driven process with the largest loss of entropy. This suggests that IgG probably undergoes more hydrophobic interactions or less structural rearrangements with plain PS-NPs, while for the functionalized NPs, hydrophilic interactions such as electrostatic interactions become more dominant. This effect is more dominant for PS-NPs-COOH than for PS-NPs-NH₂, which is in accordance with the higher net surface charge of PS-NPs-COOH (see Table I and Fig. 2). In the literature, the electrostatic interaction between negatively charged particles and immunoglobulins has already been reported.²⁷ The large heat generated between interactions of PS-NPs-COOH with IgM does not seem plausible for NP-protein interactions at first sight. In principle, it is likely that denaturation of proteins upon interaction with NCs occurs. However, such denaturation processes are endothermic and entropy-driven, which is not the case for the overall NC-Ig interactions (see Table II). Supposedly, the strong enthalpy gain is actually related to a large number of protein residues interacting with the nanoparticle surface. This is supported by the obtained stoichiometry of around 1.4 IgM molecules per NP and the fact that IgM is an immunoglobulin pentamer and thus a much larger molecule than IgG. An enthalpy gain as high as determined here would as such accordingly only be possible with a “flat-on” adsorption process of the IgM, yielding the highest available contact area. This raises the question whether the respective surface charge distribution of Igs play a role in the interactions with NPs instead of solely the overall net charge.

In order to investigate if the interactions between NPs and Igs correlate with the surface charge distribution of Igs, surface charge mapping of IgG and the F_c fragments of IgA and IgM was performed (for details, see Sec. II). The resulting surface charge distribution maps are depicted in Fig. 4.

Compared to the other Igs, IgA-F_c appears to have a relatively homogeneous distribution of charges on the surface (smaller patches). This correlates well with the relatively weak interactions of IgA with the NPs observed via SDS-PAGE and ITC. The F_c part of IgM appears to have a more heterogeneous distribution of charges (larger patches) compared to IgA. This could be an explanation for the strong (electrostatic) interactions with the strongly (negatively) charged PS-NPs-COOH, as the negative carboxyl

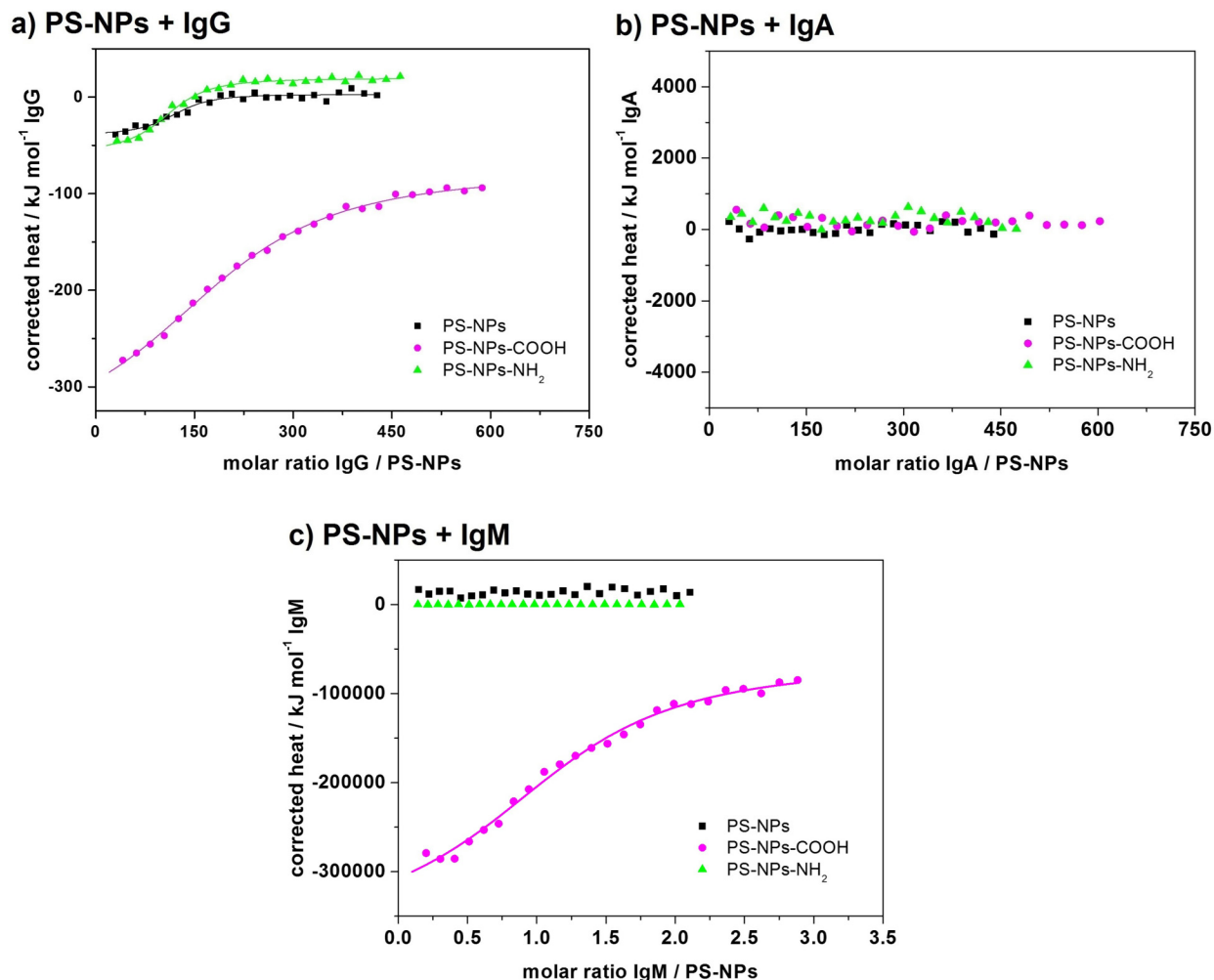


FIG. 3. Adsorption isotherms of (a) IgG, (b) IgA, and (c) IgM titrated to the different PS-NPs obtained from ITC experiments. The integrated heat of individual injections is depicted for PS-NPs (black squares), PS-NPs-COOH (pink circles), and PS-NPs-NH₂ (green triangles). Isotherms were fitted according to an independent binding model (solid lines) where possible.

TABLE II. Adsorption parameters obtained from independent binding fits of isotherms from ITC experiments.

$K_a/10^6 M^{-1}$	4.0 ± 1.0	0.41 ± 0.05	1.8 ± 0.5	2.12 ± 0.57
$\Delta H/kJ mol^{-1}$	-36 ± 5	-274 ± 34	-98 ± 19	$-353 \cdot 10^3$ $\pm 49 \cdot 10^3$
$\Delta S/J mol^{-1} K^{-1}$	-25 ± 2	-843 ± 118	-211 ± 79	$-122 \cdot 10^4$ $\pm 17 \cdot 10^4$
$\Delta G/kJ mol^{-1}$	-36.4 ± 0.6	-30.9 ± 0.3	-34.4 ± 0.7	-45.9 ± 0.6
n	121 ± 1	208 ± 18	101 ± 8	1.4 ± 0.1

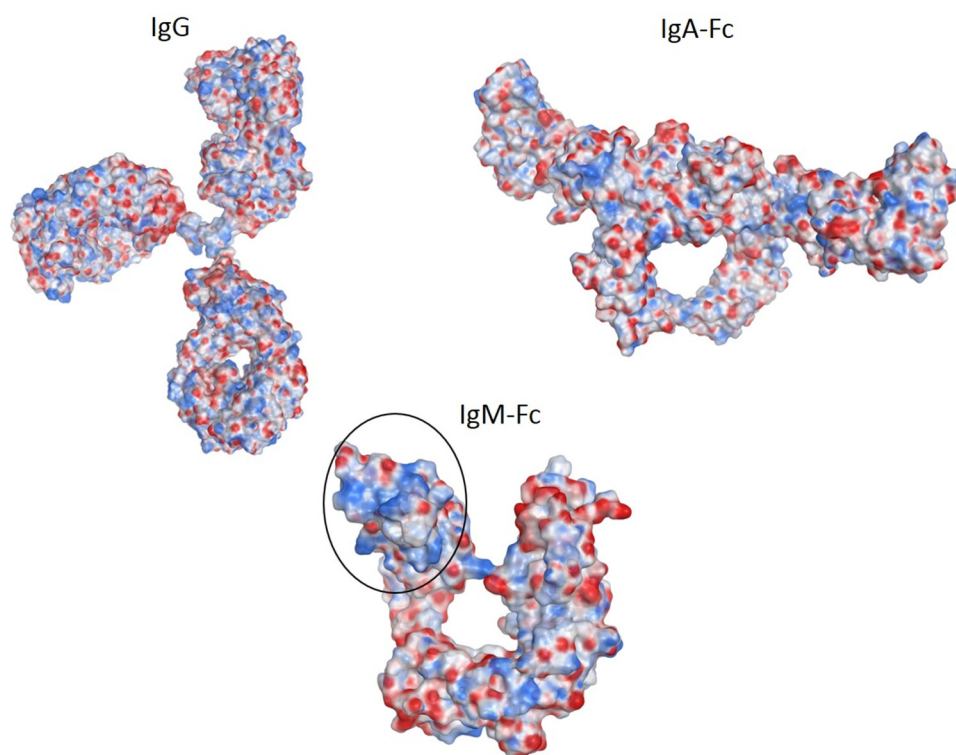


FIG. 4. Surface charge distribution maps of IgG, IgA-Fc, and IgM-Fc. Red areas in the graphics represent negatively charged patches, while blue areas represent positively charged patches and white areas are of neutral charge. One pronounced charged patch is indicated by a black circle.

groups on the NPs' surface may interact with multiple positively charged patches of IgM (see the black circle in Fig. 4).

As another possibility, bridging processes induced by the Igs could occur, which would result in aggregation of the NPs.²⁸ Accordingly, the stability of the NP-Ig complexes was analyzed via DLS (see Fig. 5) using the method by Rausch *et al.*²⁵ In brief, the autocorrelation function of all three antibodies and all three NPs are determined individually and in all NP-Ig combinations. If the sum of the autocorrelation functions of both components, with respect to the individual contribution, is sufficient to fit the data of the mixture in a so-called "forced fit," both components coexist and no aggregation processes occur. However, this "forced fit" is not capable of describing the data of the mixture in the case of aggregation events. Then, an additional term describing the diffusion behavior of the aggregate species is introduced. A more detailed description of the method is found in the supplementary material.³⁴

Following Fig. 5, larger aggregates in high concentration form in complexes between IgG and PS-NPs-COOH or PS-NPs-NH₂. All other combinations showed little amount of aggregates, which appeared to be not significant in terms of their absolute concentration. This is in accordance with the observation via SDS-PAGE and ITC that IgG interacts the strongest with the NPs, while the more electrostatic interactions with the functionalized NPs result in aggregation processes. Interestingly, no strong aggregation is observed in a mixture of PS-NPs-COOH and IgM for which strong exothermic interactions have been observed previously. It implies that this strong enthalpic interaction is not the result of

bridging processes and more likely due to electrostatic interactions between multiple (positively charged) residues of IgM with the negatively charged carboxyl groups of PS-NPs-COOH. This further highlights the influence of NPs' surface charge on the interactions with Igs.

Following the influence Igs have on the colloidal stability of NPs, the subsequent question is if NCs influence the stability of Igs in return. In a next step, we investigated if Igs appear in the (protein) corona in their native form or denature on the surface of NCs. Therefore, the stability of Igs in contact with the unfunctionalized PS-NPs was investigated via nanoDSF as an initial experiment, as these NPs showed the weakest interaction with Igs in all experiments before and are therefore most likely to show native proteins. Solutions of the native proteins served as positive controls, whereas pure PS-NPs and proteins, which were denatured by thermal treatment in a solution of SDS before the experiment, served as negative controls (see Fig. 6).

Following Fig. 6, for all native Igs, a melting point of around 65–70 °C is observed. This transition is completely lost for Igs adsorbed on PS-NPs and is very similar to the reference samples (negative controls) of Igs predenatured by treatment in SDS solution at high temperatures or PS-NPs without proteins present. To verify that enough protein was present in all samples and that the lack of a melting transition was not due to the protein amount, the peak fluorescence was investigated before each measurement (see Fig. S11).³⁴ From the peak fluorescence of each sample, it can be seen that the fluorescence of

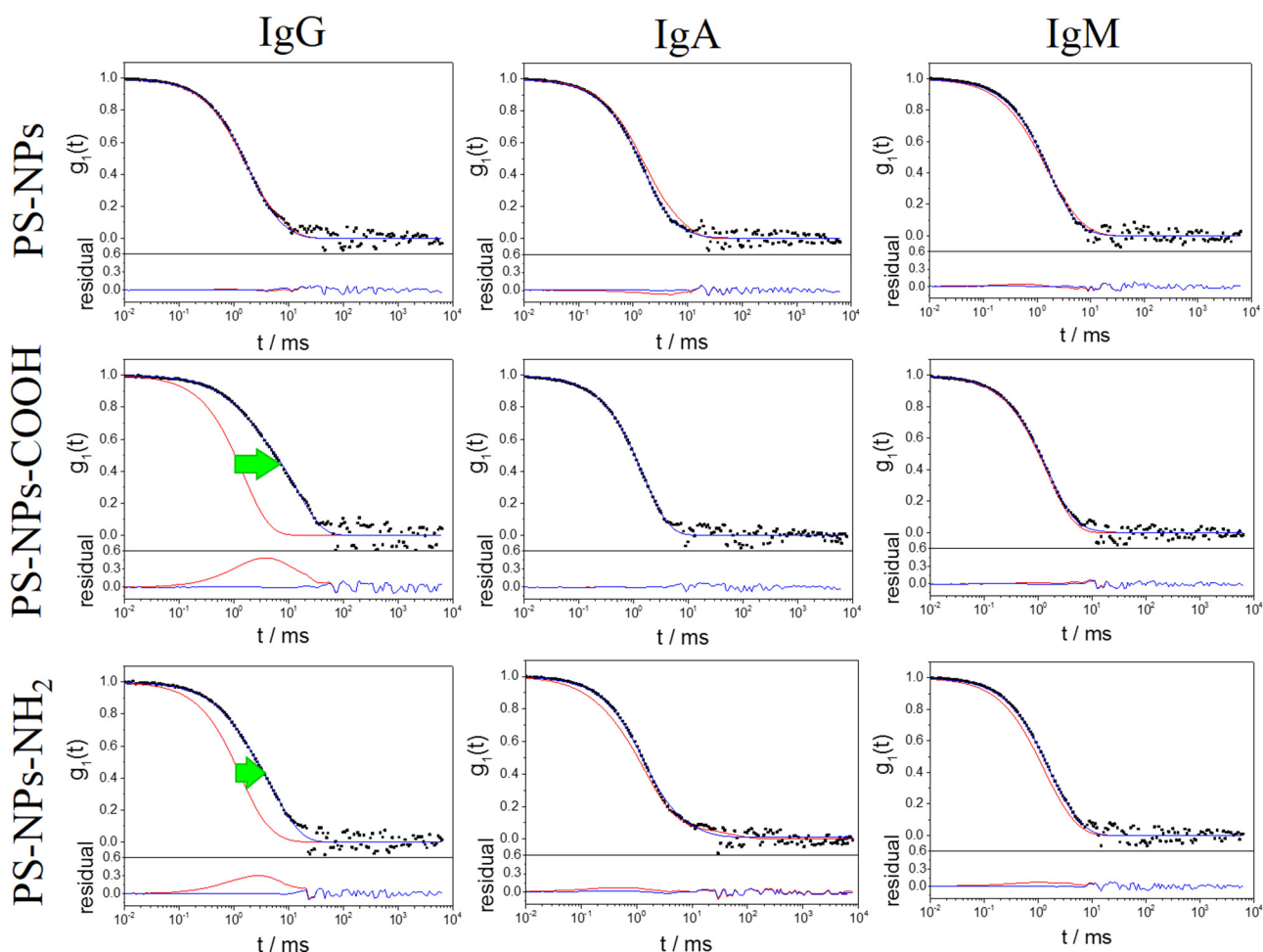


FIG. 5. DLS measurements of the different PS-NPs with IgG, IgA, and IgM. In each case of the upper graphs: autocorrelation functions $g_1(t)$ (black circles) of PS-NPs, PS-NPs-COOH, and PS-NPs-NH₂ mixed with IgG, IgA, or IgM, respectively, at $\theta = 60^\circ$. The red line represents the forced fit composed of the sum of the individual components (NPs + Igs), whereas the blue line represents the fit with an additional aggregation term. Green arrows indicate cases of severe aggregation as observed in the difference between fits with or without an additional aggregation term. Lower graphs: Corresponding residuals resulting from the difference between the data and the two fits (Scattering angle $\theta = 60^\circ$, temperature $T = 25^\circ\text{C}$).

each sample containing Igs was between the minimum and maximum fluorescence detection level of the device for a precise measurement of the melting transition. Therefore, it is confirmed that Igs were present on the surface of PS-NPs in a somewhat denatured form, as no thermal denaturation takes place during the nanoDSF experiments. This is also in line with reports for general antibody adsorption, e.g., for immunoassays where denaturation is described as very likely if adsorption occurs in an uncontrolled way.^{29,30}

These conformational changes of Igs on NPs could change cellular uptake mechanisms or induce uncontrolled reactions of the immune system as possible adverse effects. The changes occurring (partial or complete denaturation) might—along with the general aggregation of protein-nanoparticle-complexes—enhance local

aggregation of the immunoglobulins in certain areas on the particle surface. In turn, this determines the potential receptor recognition of accessible antibody F_c regions, as, e.g., monomeric IgG binds to CD64 receptors,³¹ while aggregated IgG binds to CD16/CD32.³² Additionally, locally aggregated IgG and IgM can trigger the classical pathway of the complement activation cascade,³³ so that uncontrolled immunological responses could be induced. Importantly, it has to be noted that local accumulation of immunoglobulins in the protein corona formed in full blood may also be a result of direct epitope recognition and subsequent binding and lead to similar effects as proposed by Vu *et al.*¹² This should especially be taken into account when a protein precoating strategy for nanocarriers is proposed, where further contact with additional immunoglobulins *in vivo* is unavoidable.

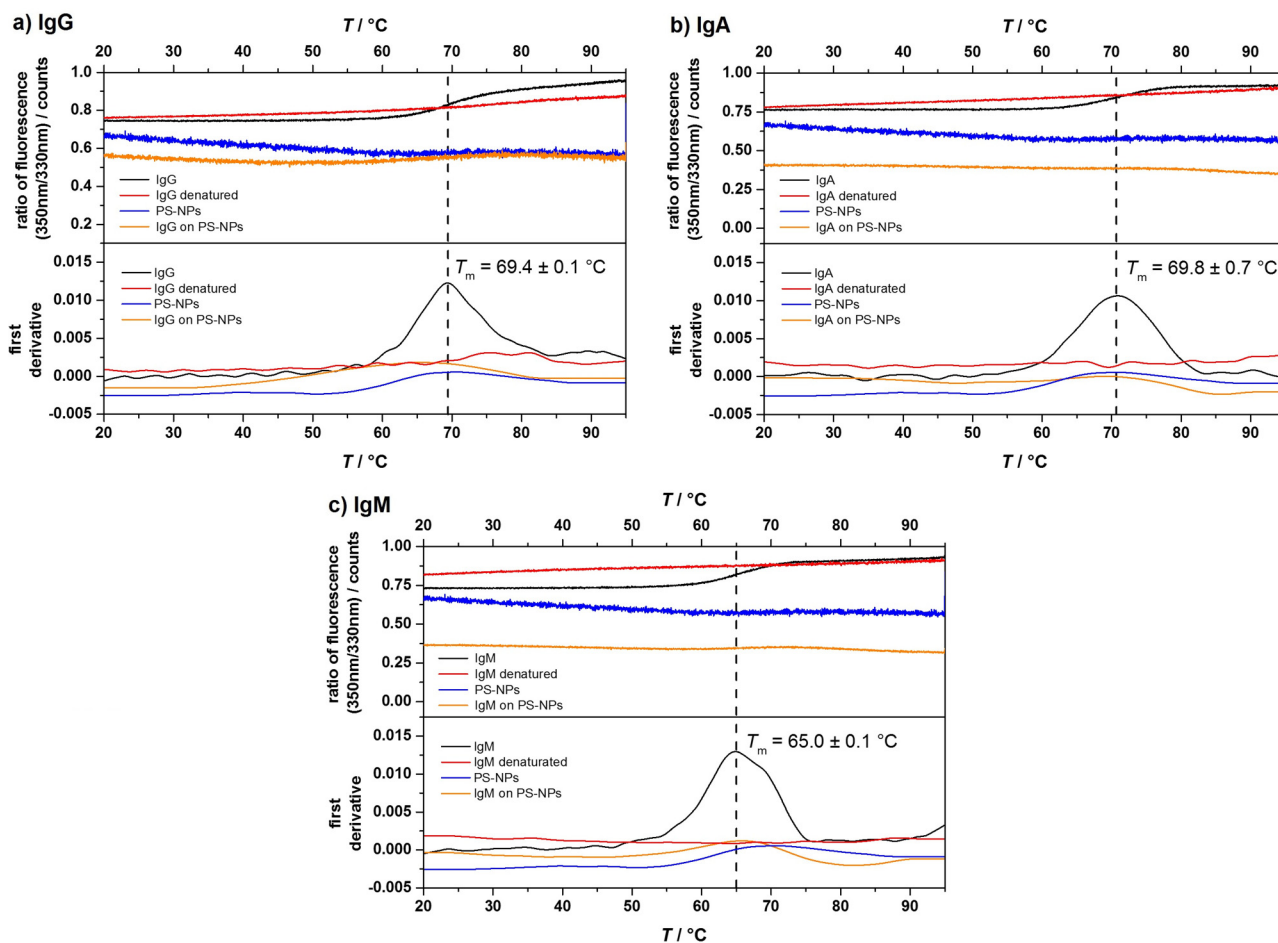


FIG. 6. NanoDSF of Igs on PS-NPs. (a) IgG, (b) IgA, and (c) IgM showing the protein unfolding (during heating up): 350/330 nm ratio of fluorescence of Igs (top) together with the first derivative (bottom). Depicted are measurements of a 1 g l^{-1} solution of the respective Ig in its native form (black line), Ig denatured by thermal treatment in 0.25 g l^{-1} SDS solution (red line), PS-NPs as negative control (blue line), and Ig on the surface of NPs after three washing steps (orange line).

Because of the above-mentioned uncertainties, in a first step, direct unspecific charge-controlled interactions between nanocarriers and immunoglobulins should be minimized, whenever possible. This highlights the importance of nanocarrier design—especially in terms of surface hydrophilicity and charge—in order to prevent unfavorable denaturation and adsorption processes of immunoglobulins on nanoparticle surfaces.

IV. CONCLUSION

In conclusion, we investigated the influence of different immunoglobulins in the protein corona of differently charged polystyrene nanoparticles. While all Igs are present on the nanoparticles' surface, Igs influence the properties of nanoparticles upon interaction and vice versa. The net charge of nanoparticles was influenced by adsorption of Igs, and aggregation processes were induced in some cases. This was particularly the case for

interactions between IgG and nanoparticles with charged functional groups. Nanoparticles with neutral surface charge exhibited less unfavorable interaction with Igs. While IgA and IgM expressed mostly weak interactions with nanoparticles, IgG underwent stronger hydrophobic interactions with unfunctionalized polystyrene nanoparticles and more hydrophilic interactions with carboxylic or amino-functionalized nanoparticles. Only for the adsorption of IgM on carboxylic nanoparticles, strong electrostatic interactions are observed, which do not result in dominant bridging and aggregation processes. Adsorption of IgG on charged nanoparticles resulted in significant aggregation. All Igs appeared to be denatured on the surface of polystyrene nanoparticles with the possible consequence of (unwanted) reactions of the immune system. From this it can be concluded that unfavorable NP-Ig interactions can be reduced by designing nanocarriers with a neutral or close to neutral net surface charge. As hydrophobic interactions play an important role in NP-Ig interactions,

forming nanocarriers of more hydrophilic materials should further minimize these interactions.

ACKNOWLEDGMENTS

The authors thank K. Klein for nanoparticle synthesis and S. L. Kuan for surface charge mapping of immunoglobulins. Additionally, they acknowledge funding from the DFG Collaborative Research Center (No. 1066).

REFERENCES

- ¹I. Lynch and K. Dawson, *Nano Today* **3**, 40 (2008).
- ²I. Lynch, A. Salvati, and K. Dawson, *Nat. Nanotechnol.* **4**, 546 (2009).
- ³G. Caracciolo, O. Farokhzad, and M. Mahmoudi, *Trends Biotechnol.* **35**, 257 (2017).
- ⁴T. Cedervall, Iseult Lynch, Stina Lindman, Tord Berggård, Eva Thulin, Hanna Nilsson, Kenneth A. Dawson, and Sara Linse, *Proc. Natl. Acad. Sci. U.S.A.* **104**, 2050 (2007).
- ⁵N. Bertrand *et al.*, *Nat. Commun.* **8**, 777 (2017).
- ⁶L. Digiacomio, F. Cardarelli, D. Pozzi, S. Palchetti, M. A. Digman, E. Gratton, A. L. Capriotti, M. Mahmoudi, and G. Caracciolo, *Nanoscale* **9**, 17254 (2017).
- ⁷M. Rahman and M. Mahmoudi, *SPIE Proc.* **9338**, 93380V (2015).
- ⁸P. M. Kelly, Christoffer Åberg, Ester Polo, Ann O'Connell, Jennifer Cookman, Jonathan Fallon, Željka Krpetić, and Kenneth A. Dawson, *Nat. Nano* **10**, 472 (2015).
- ⁹J. M. Berg, J. L. Tymoczko, and L. Stryer, *Biochemistry*, 6th ed. (Elsevier, Munich, 2007).
- ¹⁰A. Gonzalez-Quintela, R. Alende, F. Gude, J. Campos, J. Rey, L. M. Meijide, C. Fernandez-Merino, and C. Vidal, *Clin. Exp. Immunol.* **151**, 42 (2008).
- ¹¹T. Ishida, H. Harashima, and H. Kiwada, *Biosci. Rep.* **22**, 197 (2002).
- ¹²V. P. Vu *et al.*, *Nat. Nanotechnol.* **14**, 260 (2019).
- ¹³A. S. Yang, Wei Liu, Zhuoya Li, Linyu Jiang, Huibi Xu, and Xiangliang Yang, *J. Nanosci. Nanotechnol.* **10**, 622 (2010).
- ¹⁴F. Chen *et al.*, *Nat. Nano* **12**, 387 (2017).
- ¹⁵H. H. Gustafson, Dolly Holt-Casper, David W. Grainger, and Hamidreza Ghandehari, *Nano Today* **10**, 487 (2015).
- ¹⁶S. Nagayama, Ken-ichi Ogawara, Yoshiko Fukuoka, Kazutaka Higaki, and Toshikuro Kimura, *Int. J. Pharm.* **342**, 215 (2007).
- ¹⁷D. Prozeller, Jorge Pereira, Johanna Simon, Volker Mailänder, Svenja Morsbach, and Katharina Landfester, *Adv. Sci.* **6**, 1802199 (2019).
- ¹⁸J. Buijs, W. Norde, and J. W. T. Lichtenbelt, *Langmuir* **12**, 1605 (1996).
- ¹⁹C. Zhou *et al.*, *Langmuir* **20**, 5870 (2004).
- ²⁰L. Treuel, Dominic Docter, Michael Maskos, and Roland H. Stauber, *Beilstein J. Nanotechnol.* **6**, 857 (2015).
- ²¹N. C. Bell, C. Minelli, and A. G. Shard, *Anal. Methods* **5**, 4591 (2013).
- ²²V. Holzapfel, Anna Musyanovych, Katharina Landfester, Myriam Ricarda Lorenz, and Volker Mailänder, *Macromol. Chem. Phys.* **206**, 2440 (2005).
- ²³E. Hiramoto, Akihisa Tsutsumi, Risa Suzuki, Shigeru Matsuoka, Satoko Arai, Masahide Kikkawa, and Toru Miyazaki, *Sci. Adv.* **4**, eaau1199 (2018).
- ²⁴C. Thurmond, *J. Polym. Sci.* **8**, 607 (1952).
- ²⁵K. Rausch, Anika Reuter, Karl Fischer, and Manfred Schmidt, *Biomacromolecules* **11**, 2836 (2010).
- ²⁶C. Prin, Marie Christine Bene, Bernard Gobert, Paul Montagne, and Gilbert C. Faure, *Biochim. Biophys. Acta* **1243**, 287 (1995).
- ²⁷N. A. Belsey, A. G. Shard, and C. Minelli, *Biointerphases* **10**, 019012 (2015).
- ²⁸R. Cukalevski, Silvia A. Ferreira, Christopher J. Dunning, Tord Berggård, and Tommy Cedervall, *Nano Res.* **8**, 2733 (2015).
- ²⁹N. G. Welch, Judith A. Scoble, Benjamin W. Muir, and Paul J. Pigram, *Biointerphases* **12**, 02D301 (2017).
- ³⁰Y. Jung, J. Y. Jeong, and B. H. Chung, *Analyst* **133**, 697 (2008).
- ³¹R. C. van Schie and M. E. Wilson, *Clin. Diagn. Lab. Immunol.* **7**, 676 (2000).
- ³²P. D. Benech, K. Sastry, R. R. Iyer, Q. G. Eichbaum, D. P. Raveh, and R. A. Ezekowitz, *J. Exp. Med.* **176**, 1115 (1992).
- ³³C. A. Diebold *et al.*, *Science* **343**, 1260 (2014).
- ³⁴See supplementary material at <https://10.1116/6.0000139> for the SDS-PAGE experiments of Igs with and without addition of a reducing agent; data evaluation for ITC experiments; ITC raw heat rates; description of DLS data analysis; and peak fluorescence for 330 nm as observed via nanoDSF.